

Fermilab

Improved measurements of nonlinear integrable optics at IOTA

FERMILAB-CONF-23-543-AD

This manuscript has been authored by Fermi Research Alliance, LLC under Contract No. DE-AC02-07CH11359 with the U.S. Department of Energy, Office of Science, Office of High Energy Physics.

IMPROVED MEASUREMENTS OF NONLINEAR INTEGRABLE OPTICS AT IOTA

J. N. Wieland *, A. L. Romanov, A. Valishev, G. Stancari, J. D. Jarvis, Fermilab, Batavia, IL, USA
 N. Kuklev, ANL, Lemont, IL, USA
 S. Szustkowski, LANL, Los Alamos, NM, USA
 S. Nagaitsev, JLAB, Newport News, VA, USA

Abstract

Nonlinear integrable optics (NIO) are a promising novel approach at improving the stability of high intensity beams. Implementations of NIO based on specialized magnetic elements are being tested at the Integrable Optics Test Accelerator (IOTA) at Fermilab. One method of verifying proper implementation of these solutions is by measuring the analytic invariants predicted by theory. The initial measurements of nonlinear invariants were performed during IOTA run in 2019/20, however the covid-19 pandemic prevented the full-scale experimental program from being completed. Several important improvements were implemented in IOTA for the 2022/23 run, including the operation at higher beam energy of 150 MeV, improved optics control, and chromaticity correction. This report presents on the improved calibrations of the NIO for nonlinear invariant measurements.

INTRODUCTION

Contemporary particle physics experiments benefit from high intensity particle accelerators for primary beams. At high intensities, current accelerators are vulnerable to coherent instabilities. The instabilities may be mitigated by the addition on nonlinear elements for amplitude dependent detuning. Along with general lattice imperfections and higher order effects, these elements serve to reduce the available dynamic aperture. Certain configurations of NIO generate amplitude dependent detuning without impacting the stability of single particle dynamics and reducing the dynamic aperture.

IOTA is a research and development storage ring located at the Fermilab accelerator science and technology facility for studies of practical implementations of NIO. One NIO implementation in IOTA is based on static magnetic elements for a transverse, 4-D integrable system discovered by V. Danilov and S. Nagaitsev (DN) [1]. The theoretical design follows the T-insert geometry, where where symmetric drift regions with matched horizontal and vertical beta functions are separated by linear sections with an integer multiple of π phase advance. The nonlinear potential is implemented in the former drift of this linear framework. One possible resulting potential was selected for practical implementation and was used to design specialized magnetic elements for IOTA [2–4]. The theoretical 2-D potential for the DN potential [5] is given by Eq. (1), where t is the strength parameter,

Table 1: IOTA Electron Beam Parameters

Parameter	Nominal Value
Perimeter	39.96 m
Energy	150 MeV
Betatron tune, (Q_x, Q_y)	5.3
Equilibrium emittance, (ϵ_x, ϵ_y)	30 nm
RF frequency	30 MHz
Harmonic number	4
Synchrotron tune, ν_s	3.5×10^{-4}
Energy spread, σ_E	1.3×10^{-4}
Momentum compaction factor	0.083
Natural chromaticity (C_x, C_y)	-10.9, -9.4

c is the geometric parameter of the potential, and $\beta(s)$ is the beta function in the T-insert drift.

$$U(x, y) = t \operatorname{Re} \left(\frac{z}{\sqrt{1-z^2}} \arcsin(z) \right), \quad z = \frac{x + iy}{c\sqrt{\beta(s)}}, \quad (1)$$

There are two stages of the IOTA NIO research program. For the first stage, a low emittance electron beam produced in the FAST superconducting linac is used to probe the transverse phase space. Parameters of IOTA ring used during the run presented in this paper are listed in the Table 1. The second stage will switch to operation with low energy protons.

In this paper, the calibrations and verification of the DN nonlinear insert for the current IOTA run are presented.

BARE LATTICE TUNING

The requirements of the t-insert geometry place rigorous constraints on the linear lattice configuration. Before taking nonlinear measurements, the bare lattice was extensively tuned using the linear optics from closed orbits (LOCO) algorithm as implemented in Sixdsimulation [6]. The measured closed orbit offsets in the DN element are presented in Fig. 1.

The measured parameters of interest and their accuracies are included in Table 2. In addition to linear optics, chromaticity was fully compensated using two families of sextupoles.

DN ELEMENT CALIBRATION

To satisfy the DN potential, the individual elements fields must scale with the beta function. To compensate for varia-

* wielan22@msu.edu

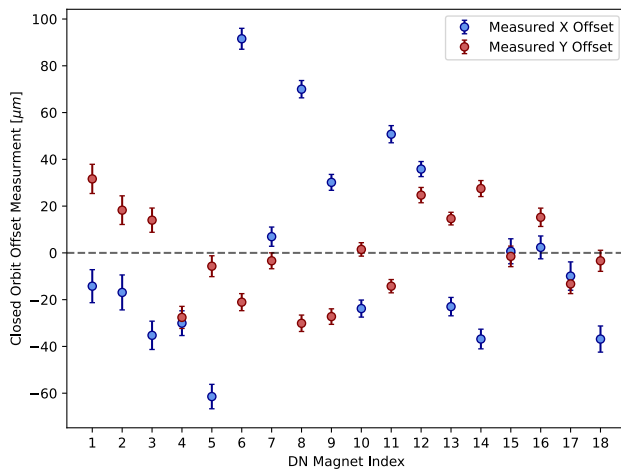


Figure 1: Closed orbit offsets in DN element.

Table 2: IOTA Bare Lattice Measurements

Bare Lattice Parameter	RMS Accuracy
Betatron Tune	1×10^{-5}
Insert Phase Advance	1×10^{-3}
Insert Orbit Centering	50 μm
Chromaticity (C_x, C_y)	0.03, 0.06

tions between the magnets, the 18 individual magnets were calibrated with beam based measurements. The multipole expansion of the nonlinear magnetic field is given in Eq. (2). Here $B\rho$ is the beam rigidity, and $t, c, \beta(s)$ are the same factors as in Eq. (1).

$$B_y + iB_x = -t \frac{B\rho}{\beta(s)} \sum_{n=1}^{\infty} \frac{2^{2n-1} n! (n-1)! c}{(2n-1)! \sqrt{\beta(s)}} \left(\frac{x + iy}{c\sqrt{\beta(s)}} \right)^{2n-1} \quad (2)$$

At small amplitudes the quadrupole term dominates. This was verified with measurements of tune dependence on kick amplitude for a single excited magnet. To determine the individual calibration, the quadrupole tune shift due to the first order term is set equal to the measured value and solved for necessary t-scaling, Eq. (3).

$$\Delta Q_{x,y} = \pm \frac{1}{4\pi} \int \beta(s) \frac{\Delta B_2}{B\rho} ds, \quad \Delta B_2 = \frac{-2B\rho \Delta t}{\beta^2(s)} \quad (3)$$

Each magnet was energized individually and a small amplitude kick was applied to the beam to measure the tune shift. This was done for multiple current setpoints to fit a tune shift vs current. Tune was measured by applying the NAFF algorithm to kicked turn-by-turn bpm data [7]. The resulting data gives a current scaling profile for the overall insert Fig. 2.

NONLINEAR TUNE SHIFT

The DN insert nonlinear detuning was measured to verify calibration. The theoretical detuning is given in Eq. (4) [8].

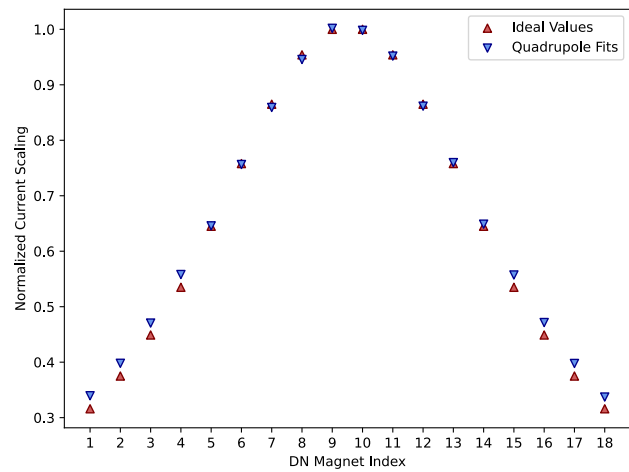


Figure 2: Normalized DN insert current scaling profile compared to calculated ideal values.

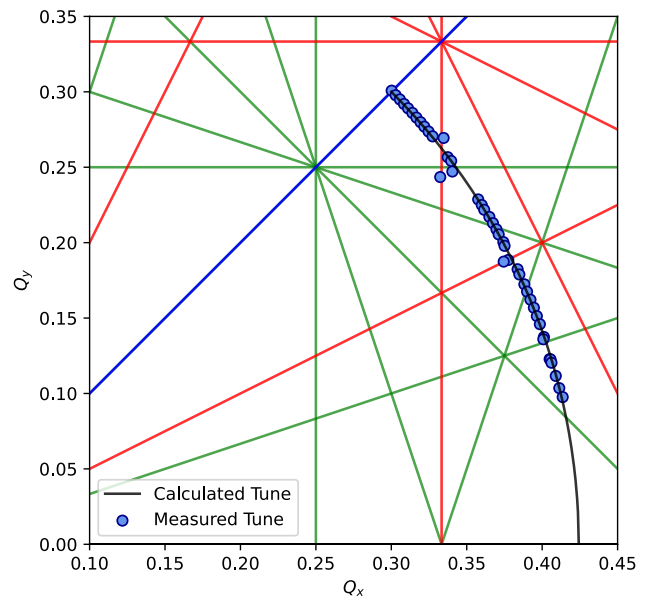


Figure 3: Nonlinear detuning on resonance diagram.

$$\begin{aligned} Q_x &= Q_o \sqrt{1 + 2t} \\ Q_y &= Q_o \sqrt{1 - 2t} \end{aligned} \quad (4)$$

The detuning was measured by adjusting the t-parameter of the entire DN insert and kicking the beam for a turn-by-turn tune measurement. The results plotted along with the calculated ideal detuning are presented in Fig. 3.

The detuning ratio between the planes supports proper implementation of the potential. The absolute t-parameter scaling may be verified by investigating detuning vs nominal t-parameter, Fig. 4.

The initial data indicated a discrepancy in the tune dependence of the t-parameter. The proportionality between the horizontal and vertical tunes (Fig. 3) showed no significant aberrations, which pointed to the absolute scaling of the

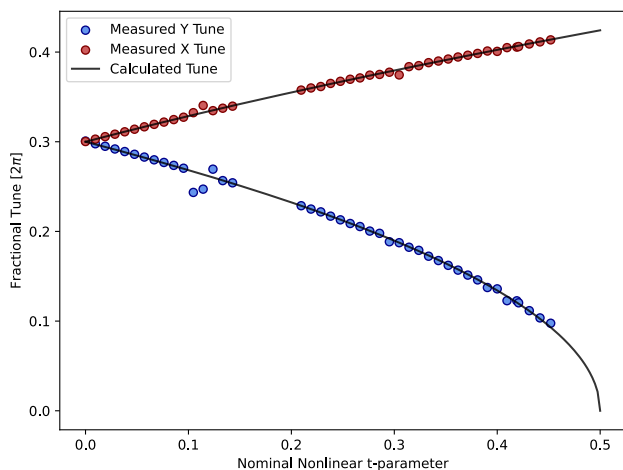


Figure 4: Detuning vs t-parameter in both planes, gap in data between $t=0.1$ and 0.2 was due to error in data acquisition system, t-parameter of measured data is scaled by 0.935 from fit.

t-parameter. The ideal detuning expression was fit to the data with a t-scaling factor as the only free parameter Eq. (5).

$$Q = Q_o \sqrt{1 \pm 2at} \quad (5)$$

This indicated that the calibrated t-parameter scaling was $a \approx 0.935$ of the nominal t-parameter. The source of this discrepancy is not yet clear, but is suspected to be a combined effect of the entire insert since the calibration was measured with single elements.

The impact of the strong sextupoles implemented to compensate chromaticity can be seen in Fig. 3 as the dominant effect on the tune near the third order resonances (red lines on tune diagram).

LOSSES SCAN

A final verification of the implementation was performing a scan of the t-parameter and logging the beam current to determine losses, Fig. 5.

The largest losses can be seen at the t-parameters corresponding to crossing the horizontal third order resonance. The third order resonances show some improvement over the 2019/2020 run where a sextupole scaling scheme had to be implemented in order to cross these resonances without 90% beam loss if they were energized. In practical operation, this is not an issue as losses are negligible if the resonance is crossed quickly. Additional losses are observed at a t-parameter of 0.46. There are several higher order resonances which may drive losses at this point but the exact source is not clear. There are no significant losses observed at the integer resonance.

CONCLUSION

The bare lattice and DN NIO insert in IOTA have been calibrated and verified for studies. Data collection for calcu-

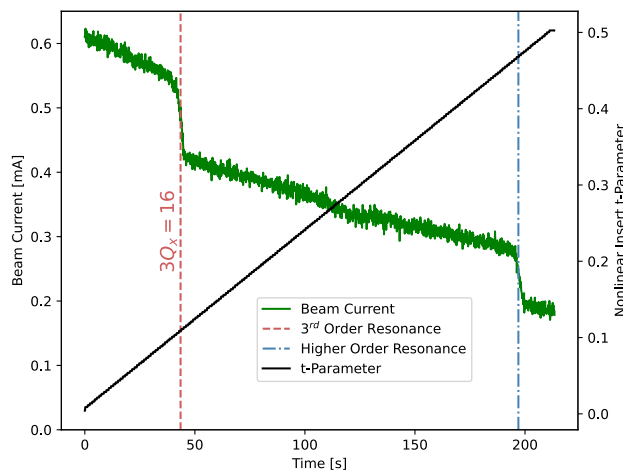


Figure 5: Beam current for t-parameter scan.

lation of the nonlinear invariants from reconstructed turn-by-turn phase space is now ongoing.

REFERENCES

- [1] V. Danilov and S. Nagaitsev, "Nonlinear accelerator lattices with one and two analytic invariants," *Phys. Rev. Spec. Top. Accel Beams*, vol. 3, p. 084002, 2010. doi:10.1103/PhysRevSTAB.13.084002
- [2] F. H. O'Shea, R. B. Agustsson, A. Y. Murokh, and E. Spranza, "Measurement of Non-Linear Insert Magnets", in *Proc. NAPAC'13*, Pasadena, CA, USA, Sep.-Oct. 2013, paper WEPBA17, pp. 922–924.
- [3] F. O'Shea, R. Agustsson, Y.-C. Chen, D. Martin, J. McNevin, and E. Spranza, "Non-linear Magnetic Inserts for the Integrable Optics Test Accelerator", in *Proc. IPAC'15*, Richmond, VA, USA, May 2015, pp. 724–727. doi:10.18429/JACoW-IPAC2015-MOPMN010
- [4] F. H. O'Shea, R. B. Agustsson, P. S. Chang, and Y. C. Chen, "Non-Linear Inserts for the IOTA Ring", in *Proc. IPAC'17*, Copenhagen, Denmark, May 2017, pp. 4407–4409. doi:10.18429/JACoW-IPAC2017-THPIK129
- [5] C. Mitchell, "Complex representation of potentials and fields for the nonlinear magnetic insert of the integrable optics test accelerator," *arXiv*, 2019. doi:10.48550/arXiv.1908.00036
- [6] A. Romanov, D. Edstrom Jr., F. A. Emanov, I. A. Koop, E. A. Perevedentsev, Y. A. Rogovsky, D. B. Schwartz, and A. Valishev, "Correction of magnetic optics and beam trajectory using LOCO based algorithm with expanded experimental data sets," *arXiv*, Mar. 2017. doi:10.48550/arXiv.1703.09757
- [7] P. Zisopolous, Y. Papahilippou, and J. Laskar, "Refined betatron tune measurements by micking beam position data," *Phys. Rev. Spec. Top. Accel Beams*, vol. 22, p. 071002, 2019. doi:10.1103/PhysRevAccelBeams.22.071002
- [8] S. Nagaitsev, A. Valishev, and V. Danilov, "Nonlinear optics as a path to high-intensity circular machines," *arXiv*, July 2012. doi:10.48550/arXiv.1207.5529